water

MDPI

Article

Wavelet-ANN versus ANN-Based Model for Hydrometeorological Drought Forecasting

Md Munir H. Khan [1,2], Nur Shazwani Muhammad [1,*] and Ahmed El-Shafie [3]

1 Smart and Sustainable Township Research Centre, Faculty of Engineering and Built Environment, Universiti Kebangsaan Malaysia (UKM), Bangi 43600, Selangor Darul Ehsan, Malaysia; shihab.bd@gmail.com
2 Faculty of Engineering & Quantity Surveying, INTI International University (INTI-IU), Persiaran Perdana BBN, Putra Nilai, Nilai 71800, Negeri Sembilan, Malaysia
3 Department of Civil Engineering, Faculty of Engineering, University of Malaya (UM), Kuala Lumpur 50603, Malaysia; elshafie@um.edu.my
* Correspondence: shazwani.muhammad@ukm.edu.my; Tel.: +60-3-8921-6226

Received: 4 June 2018; Accepted: 10 July 2018; Published: 27 July 2018

Abstract: Malaysia is one of the countries that has been experiencing droughts caused by a warming climate. This study considered the Standard Index of Annual Precipitation (SIAP) and Standardized Water Storage Index (SWSI) to represent meteorological and hydrological drought, respectively. The study area is the Langat River Basin, located in the central part of peninsular Malaysia. The analysis was done using rainfall and water level data over 30 years, from 1986 to 2016. Both of the indices were calculated in monthly scale, and two neural network-based models and two wavelet-based artificial neural network (W-ANN) models were developed for monthly droughts. The performance of the SIAP and SWSI models, in terms of the correlation coefficient (R), was 0.899 and 0.968, respectively. The application of a wavelet for preprocessing the raw data in the developed W-ANN models achieved higher correlation coefficients for most of the scenarios. This proves that the created model can predict meteorological and hydrological droughts very close to the observed values. Overall, this study helps us to understand the history of drought conditions over the past 30 years in the Langat River Basin. It further helps us to forecast drought and to assist in water resource management.

Keywords: drought analysis; ANN model; drought indices; meteorological drought; SIAP; SWSI; hydrological drought; discrete wavelet

1. Introduction

Drought gradually happens with a lack of rainfall for a long period of time (i.e., months or years). This natural disaster is considered to be the most complex and least understood by many scientists. The impact of drought varies with respect to the affected areas. The damage may include impacts on the social and agriculture sectors, and the economy [1]. In 2007, it was reported that, because of the tremendously hot temperature, heat waves, and heavy rainfalls, extreme events would accumulate and become more frequent [2]. Although Malaysia experiences a tropical climate and receives more than 2000 mm of total rainfall annually, over the recent years, the country has experienced several drought episodes. For example, the state of Melaka faced a serious water shortage when water levels in the dams fell under critical levels in 1991, and the Durian Tunggal dam, which serves as a major water supply dam, ran dry [3]. In 1998, an El Nino-related drought severely hit the states of Selangor, Kedah, and Penang, which caused severe social and environmental impacts across the country [3]. This drought caused water rationing and hardship for 1.8 million residents of Kuala Lumpur and other towns in Klang Valley.

The Langat River Basin also experienced a rise in temperature nearly 5° higher than usual on many days in March and April 2016 [4]. A research study applied the standardized precipitation index (SPI) to evaluate dry conditions using the data from 10 gauging stations throughout peninsular Malaysia, and found that extreme dry conditions are becoming more frequent than extreme wet conditions [5]. Thus, emphasis should be placed on measures to reduce the impact of dry conditions, although the authorities usually put more focus on reducing extreme wet conditions (i.e., floods).

Drought is generally analyzed by means of drought indices, which are effectually a function of precipitation and other hydrometeorological variables [6]. Different drought indices have been discovered and are used in different nations [6]. Hydrologists have defined four major categories of drought, namely, meteorological drought, agricultural drought, hydrological drought, and socioeconomic drought [1]. Drought monitoring by indices in specific areas must be based on the availability of hydrometeorological data and the capability of the index to dependably detect spatial and temporal differences through a drought event. Nevertheless, no single indicator or index alone can precisely describe the onset and severity of the event. Numerous climate and water supply indices are used to describe the severity of any drought event. Although none of the major indices is inherently superior to the rest in all circumstances, some indices are better suited for certain uses than others [7]. In this study, the first objective was to assess the drought using two drought indices (DIs), the Standard Index of Annual Precipitation (SIAP) and the Standardized Water Storage Index (SWSI), to represent meteorological and hydrological droughts, respectively. The SIAP and SWSI were chosen for their simplicity, and they do not require parameter estimation. Gourabi [8] used SIAP and the dependable rainfall index (DRI) for the recognition of drought years in several areas in Iran, and to analyze the effects on rice yield and water surface. Sing et al. [9] used SIAP and a few other indices to assess the drought spells in the Almora district of Uttarakhand, India. On the other hand, to calculate SWSI, the Standardized Drought Assessment Toolbox (SDAT), developed by Farahmand and AghaKouchak in 2015 [10], is used. The SDAT methodology standardizes the marginal probability of drought-related variables (e.g., precipitation, soil moisture, and relative humidity) using the empirical distribution function of the data. This approach does not require an assumption of the representativeness of a parametric distribution function to describe drought-related variables. Additionally, the nonparametric framework does not require a parameter estimation and goodness-of-fit evaluation, which makes the SDAT framework computationally much more efficient. Wang et al. [11] used four drought indices, including SWSI, in order to assess the intensity and timing of drought events in the upper and middle Yangtze River Basin in China. In the second objective of this study, artificial neural network (ANN)–based models coupled with a wavelet were developed and their performance evaluation was carried out for both SIAP and SWSI models.

Many researchers have developed and applied various models to predict hydrological events, which could be divided into two major types, conceptual models (CM) and data-based models (DDM) [12]. The conceptual models usually incorporate simplified schemes of physical laws and are generally nonlinear, time-invariant, and deterministic, with parameters that are representative of watershed characteristics. However, when they are calibrated to a given set of hydrological signals (time series), there is no guarantee that the conceptual models can predict accurately when they are used to extrapolate beyond the range of calibration or verification experience [13,14]. It was also a bit difficult to understand the nature of these kind of models, so, in order to use such kind of models it was very important that, in order to get better results, one should have all of the knowledge about the models and its parameters [15]. However, DDM, which are basically numerical and based on biological neuron systems, recently known as an artificial brain or intelligence, have received more attention in water related applications because of their ease, fast progress time, and less data necessity. The ANN- or data-driven models have become increasingly popular in hydrologic forecasting because they are effective at dealing with the nonlinear characteristics of hydrological data [16]. Among the various machine learning methods, artificial neural networks (ANNs), which include back-propagation neural network (BPNN), radial basis function (RBF) neural network, generalized regression neural network (GRNN), Elman

neural network, and multilayer feed-forward (MLFF) network, are among the most popular techniques for hydrological time series forecasting [17]. Although data driven models have attained high levels in the hydrological field, there is still space present to improve the forecasting methods [18]. Hydrological processes are non-linear and arbitrary. By simply applying such models on an original time series, the facts of alteration are overlooked, so that prediction correctness is reduced [19].

In the last decade, wavelet transform has become a widely applied technique for analyzing variations, periodicities, and trends in time series [20,21]. Wavelet transform, which can produce a good local representation of the signal, in both the time and frequency domains, provides considerable information on the structure of the physical process to be modelled. Discrete wavelet transformation provides a decomposition of original time series. Subseries decomposed by discrete wavelet transform, from original time series, provide detailed information about the data structure and its periodicity [22]. The attributes of each subseries are different. The wavelet components of the original time series improve on a forecasting model by giving useful information on various resolution levels [23]; however, not much research has applied a wavelet for drought forecasting. A major limitation of artificial neural networks (ANNs) is their inability to deal with nonstationary data. To overcome this limitation, researchers have increasingly begun to use a wavelet analysis to preprocess the inputs of the hydrologic data. Shabri [24] proposed a hybrid wavelet–least square support vector machine (WLSSVM) model that combines the wavelet method and the LSSVM model for monthly stream flow forecasting. Belayneh and Adamowski [25] studied drought forecasting using machine learning techniques and found that coupled wavelet neural network models were the most accurate for forecasting three month SPI (SPI 3) and six month SPI (SPI 6) values over lead times of one and three months in the Awash River Basin in Ethiopia. Therefore, in this study, coupling wavelets with ANN was expected to provide significant improvements in the model performance.

2. Materials and Methods

2.1. Standard Index of Annual Precipitation (SIAP)

The SIAP is known for transferring the raw data of precipitation to relative amounts, so that the deviation of rainfall from mean can be divided to standard deviation. Khalili [26] developed the SIAP and applied it to the study the processes of drought and wet conditions in Iran [27]. The values of the SIAP can be computed by Equation (1), provided by Khalili [6,26], as follows:

$$\mathrm{SIAP} = \frac{\mathrm{P_i} - \overline{\mathrm{P}}}{\mathrm{PSD}} \quad (1)$$

where SIAP is the drought index, $\mathrm{P_i}$ is the annual precipitation, P is the mean of precipitation in the period, and PSD is the standard deviation of the period. SIAP classifies drought intensity into five major categories, namely, extremely wet, wet, normal, drought, and extreme drought. Details on the SIAP classifications are given in Table 1 [9,27].

In this study, SIAP is applied for short-term/monthly drought analysis. The pattern of the raw rainfall data shows a normal distribution, which supports the concept behind using SIAP on a short-term/monthly scale. Hence, Equation (1) is rewritten as follows:

$$\mathrm{SIAP\ (M)} = \frac{\mathrm{P_i} - \overline{\mathrm{P}}}{\mathrm{SD}}$$

where SIAP (M) is the drought index on a monthly time scale, $\mathrm{P_i}$ is the monthly rainfall in the $\mathrm{i^{th}}$ month (i = 1, 2, 3, 4, ... 360), P is the mean of the monthly rainfall data for the whole period of study, and SD is the standard deviation of the monthly rainfall for the duration of the study.

Table 1. Classification of Standard Index of Annual Precipitation (SIAP) values.

Classes of Drought Intensity	SIAP Values
Extremely wet	0.84 or more
Wet	0.52 to 0.84
Normal	−0.52 to 0.52
Drought	−0.52 to −0.84
Extreme drought	−0.84 or less

2.2. Standardized Water Storage Index (SWSI)

The SWSI is used to assess the deficit in the terrestrial water reserves. The SWSI calculation is based on Equation (2). It is calculated by the SDAT toolbox in MATLAB, which was developed by Farahmand and AghaKouchak [10].

$$SWSI_{i,j} = \frac{S_{i,j} - S_{j,mean}}{S_{j,sd}} \quad (2)$$

where $S_{i,j}$ is the seasonal water level for year i and month j, $S_{j,mean}$ is the mean water level of the corresponding month for the duration of the study, and $S_{j,sd}$ is the standard deviation. The details of SWSI classification are given in Table 2.

Table 2. Classification of the Standardized Water Storage Index (SWSI).

SWSI Values	Classification
2.0 or more	Extremely wet
1.5 to 1.99	Very wet
1.0 to 1.49	Moderately wet
−0.99 to 0.99	Near normal
−1.49 to −1.00	Moderate drought
−1.99 to −1.5	Severe drought
−2 or less	Extreme drought

2.3. Development of Forecasting Model Using ANN

An artificial neural network can be defined as a set of simple processing units working as a parallel distributed processor [28]. These units, which are called neurons, are responsible for storing experimental knowledge for later disposal. The ANNs mimic the biological nervous system, similar to the brain; they learn through examples and have acquired knowledge stored in the connection weights between neurons [29]. The data are introduced in the input layer and the network progressively processes the data through the subsequent layers, producing a result in the output layer. The input neurons are linked to those in the intermediate layer through w_{ji} weights, and the neurons in the intermediate layer are linked to those in the output layer through w_{ki} weights. The symbols i, j, and k represent the ith, jth, and kth neuron in input, hidden, and output layers, respectively. The network maps out the relation between the input data and the output variables based on the nonlinear activation functions. The purpose of training a network is to minimize the error between outputs of the network and the target values. The training algorithm reduces the error by adjusting the weights and biases of the network. In training, the input values are multiplied by the respective connection weights and then the biases are added. The same process is repeated for the output layer, where the output of a hidden layer is used as an input the output layer. The combination of net weighted input and biases net_j to the jth neuron of the hidden layer can be expressed as [30] follows :

$$net_j = \sum_{i=1}^{l} (w_{ji} x_i + b_j) \quad (3)$$

where x_i is the input value to the ith neuron of the input layer, while w_{ji} is the weight of the jth neuron of the hidden layer connected to the ith neuron of the input layer, and b_j is the bias of the jth hidden neuron. The net value, net_j, is passed through a transfer or activation function in the hidden layer to produce an output from the hidden neuron. The output from the hidden layer can be expressed as [30] follows:

$$y_j = f(net_j) = f_h\left(\sum_{i=1}^{p}(w_{ji}x_i + b_j)\right) \tag{4}$$

where y_j is the output from the jth hidden neuron. The output from the hidden layer, y_j, is used as an input to the output layer, and the same process as in hidden layer is repeated in the output neurons in order to produce an output from the output layer. The net weighted input to the output neuron can be represented by [30] the following:

$$net_k = \sum_{j=1}^{q} f_o(y_j)w_{ki} + b_k \tag{5}$$

Similar to above, the output from the kth neuron in the output layer is given by [30] the following:

$$y_k = f(net_k) = f_o\left(\sum_{j=1}^{q} w_{ki}f_h\left(\sum_{i=1}^{p}(w_{ji}x_i + b_j)\right) + b_k\right) \tag{6}$$

The ANN weights are made and modified iteratively through a procedure called calibration. The ANN models used in this study have a feed-forward multilayer perceptron (MLP) architecture that was trained with the Levenberg–Marquardt (LM) back-propagation algorithm. MLPs have often been used in hydrologic forecasting because of their simplicity. MLPs consist of an input layer, one or more hidden layers, and an output layer. The Levenberg–Marquardt (LM) algorithm is used for training because it is considered one of the fastest methods for training ANNs. The major drawback of feed-forward network models, as used in this study, is their inability to mimic the temporal pattern trend during the model training stage. Therefore, this type of model may not be capable of providing a reliable and accurate forecasting solution [31]. The efficiency of the models may be assessed using several statistical parameters, which describe the adhering degree among the data that are observed and predicted by the model [32,33]. A neuron computes and gives feedback based on the weighted sum of all of its inputs, according to an activation function based on its output [34]. The activation function selected here is the sigmoidal activation function. Standard neural network training procedures adjust the weights and biases in the network to minimize a measure of 'error' in the training cases, which is most commonly the sum of the squared differences between the network outputs and the targets. Finding the weights and biases that minimize the chosen error function is commonly done by using some gradient-based optimization method, with derivatives of the error, with respect to the weights and biases calculated by back-propagation. A detailed theory of the back-propagation algorithm is beyond the scope of this research and can be found in Haykin [28]. In this study, the Neural Networks Toolbox of MATLAB® is used. Figure 1 shows a simple neural network structure.

The performance of the presented models is evaluated based on their correlation coefficient (R) and root mean-square error (RMSE). The estimation of R is done using Equation (7), as follows:

$$\mathrm{R} = \frac{\frac{1}{n}\sum_{t=1}^{n}\left(y_t^o - \overline{y}_t^o\right)\left(y_t^f - \overline{y}_t^f\right)}{\sqrt{\frac{1}{n}\sum_{t=1}^{n}(y_t^o - \overline{y}_t^o)^2}\sqrt{\frac{1}{n}\sum_{t=1}^{n}\left(y_t^f - \overline{y}_t^f\right)^2}} \tag{7}$$

where y_t^o and y_t^f are the observed and forecasted values at time t, respectively, and n is the number of data points.

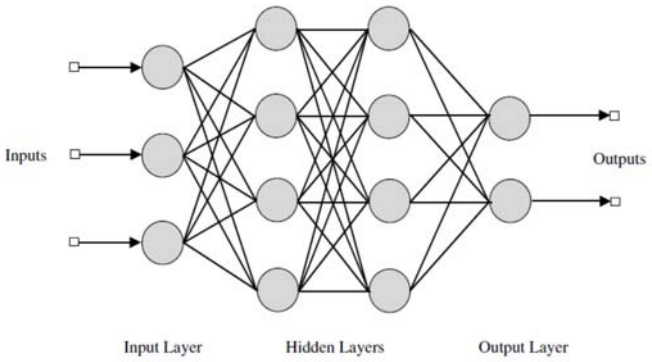

Figure 1. Neural network structure.

The correlation coefficient (R) measures how well the predicted values correlate with the observed values and shows the degree to which the two variables are linearly related. An *R* value close to unity indicates a satisfactory result, while a low value or one that is close to zero implies an inadequate result.

The RMSE provides information about the predictive capabilities of the model. The RMSE evaluates how close the predictions match the observations, shown in Equation (8), as follows:

$$\text{RMSE} = \sqrt{\frac{1}{n}\sum_{t=1}^{n}\left(y_t^o - y_t^f\right)^2} \tag{8}$$

The criteria for deciding the best models are based on how small the RMSEs found in training, testing, and validation of the data are.

2.4. Discrete Wavelet

Wavelet analysis is a multi-decomposition analysis that provides information on both the time and frequency domains of the signal, and is the important derivative of the Fourier transform. The wavelet will become an important tool in time series forecasting. The basic objective of wavelet transformation is analyzing the time series data, in both the time and frequency domains, by decomposing the original time series in different frequency bands using wavelet functions. Compared to the Fourier transform, time series are analyzed using sine and cosine functions. Wavelet transformations provide useful decompositions of the original time series by capturing useful information on various decomposition levels.

Nowadays, wavelet analysis is one of the most powerful tools in the study of time series. Wavelet transform can be divided into two categories, continuous wavelet transform (CWT) and discrete wavelet transform (DWT). CWT is not often used for forecasting because of its computational complexity and time requirements [35]. Among the reviewed papers by Nourani et al., [36], only about 20% of the studies used the CWT for decomposing the hydrological time series, and the majority of studies utilized the DWT. This is because real world observed hydrologic time series are measured and gathered in discrete form, rather that in a continuous format [36]. DWT is often used in forecasting applications to simplify numeric solutions. DWT requires less computation time and is simpler to apply. DWT is given by the following:

$$\psi_{m,n}(t) = \frac{1}{\sqrt{s_o^m}}\ \psi\left\{\frac{t - n\tau_o s_o^m}{s_o^m}\right\} \tag{9}$$

where $\psi\,(t)$ is the mother wavelet, and m and n are integers that control the scale and time, respectively. The most common choices for the parameters are $S_o = 2$ and $\tau_o = 1$. According to Mallat's theory,

the original discrete time series can be decomposed into a series of linearity-independent approximation and detail signals, by using the inverse DWT. The inverse DWT is given by Mallat [37], as follows:

$$x(t) = T + \sum_{m=1}^{M} \sum_{t=0}^{2^{M-m-1}} W_{m,n}\, 2^{-\frac{m}{2}} \psi\left(2^{-m}\, t - n\right), \tag{10}$$

where $W_{m,n} = 2^{-\frac{m}{2}} \sum_{t=0}^{N-1} . \psi(2^{-m}\, t - n)x(t)$ is the wavelet coefficient for the discrete wavelet at scale $s = 2^m$ and $\tau = 2^m\, n$.

2.5. W-ANN Model

The W-ANN model is obtained by combining the DWT and ANN models. The W-ANN model uses the subseries obtained from using DWT on original data. The W-ANN model structure developed in this study can be described with the following steps:

1. Decompose the original time series for each input into subseries components (details and approximations) by DWT.
2. Select the most important and effective of each subseries component for each input by the correlation coefficient.
3. Construct a W-ANN model using the new summed series obtained by adding the significant components of details sub-time series and approximations sub-time series for each input as the new input to the ANN, and the original output time series as the output of the ANN. Figure 2 shows a schematic representation of the model.

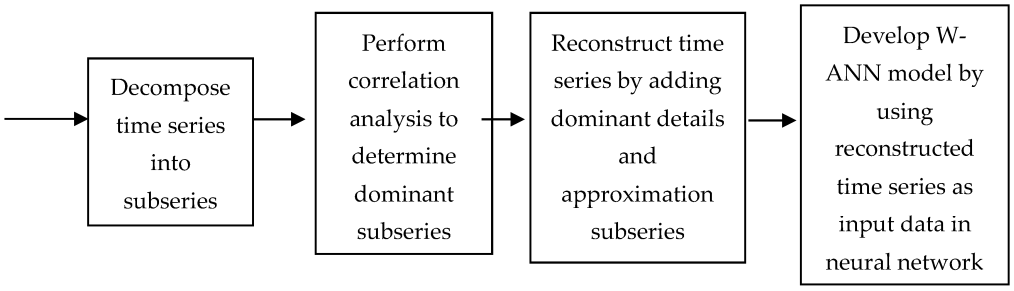

Figure 2. Schematic diagram of wavelet-based artificial neural network (W-ANN) model development.

2.6. Study Area and Data Collection

2.6.1. Langat River Basin

The Langat River is situated in the state of Selangor, Malaysia. This river basin is located near Kuala Lumpur, the capital city of Malaysia. Therefore, the study area has been rapidly developed, which makes it dependent on the Langat River for water supply [38]. The Langat River has an estimated total catchment area of 1817 km^2 and is located at latitude 2°40′152″ N to 3°16′15″ N and longitude 101°19′20″ E to 102°1′10″ E [30], and the main river is 141 km in length. The Beranang River, Semenyih River, and Lui River are the main tributaries of the Langat River, as shown in Figure 3. There are two reservoirs in the Langat River Basin, Hulu Langat and Semenyih. The northeastern part of the river basin has a reduced level (RL) of 960 m above the mean sea level and is mountainous. The temperature of the area varies from 23.5 °C to 33.5 °C all year, and the comparative humidity ranges from 63% to 95%, with an average of 81%. Heavier rainfall happens in the month of November, with a monthly average rainfall of 270 mm; the average annual rainfall of the study area is about 2400 mm [38]. The area also sometimes experiences rainstorms, and these usually occur in the early evening through the year, and are usually of a short duration with a high intensity.

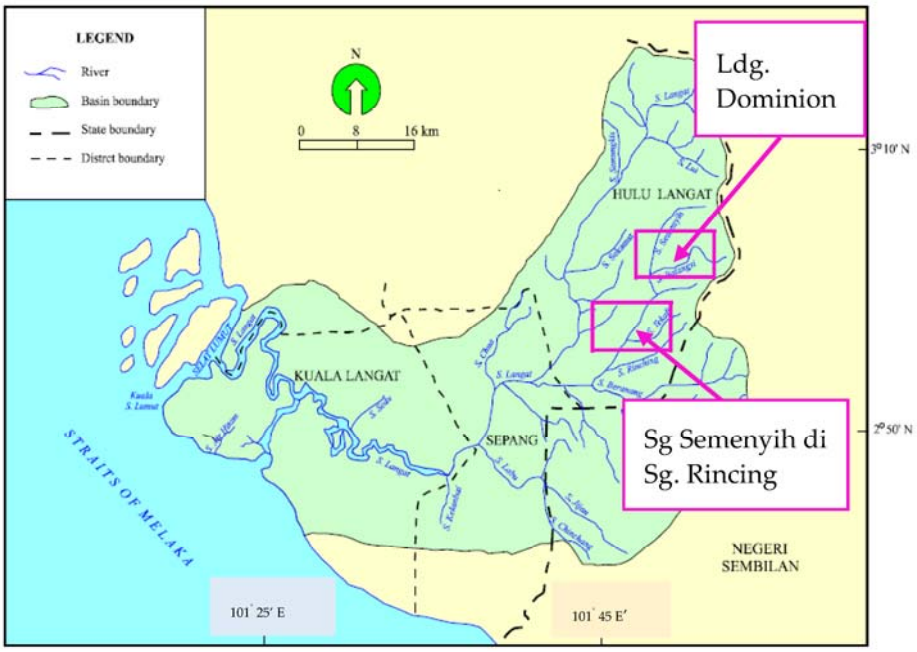

Figure 3. Langat River Basin.

2.6.2. Data Collection

Thirty years (1986–2016) of rainfall and water level data of stations were collected from the Department of Irrigation and Drainage (DID), Malaysia. Table 3 gives details of the gauging stations, including the station name, station number, coordinates (latitude and longitude), data availability, and percentage of missing data.

Table 3. Details on rainfall and water level gauging stations.

Station	Station Name	Station No.	Coordinates		Data Availability (Years)	Missing Data (%)
			Latitude (N)	Longitude (E)		
1	Sg. Semenyih di Sg. Rincing	WL 2918401	02°54′55″	101°49′25″	1986–2016	5.4%
2	Ldg. Dominion	RF 3018107	03°00′13″	101°52′55″		6.5%

For the simplicity of naming the stations, water level (WL) station Sg. Semenyih di Sg. Rincing (WL 2918401) will be referred as station 1, and rainfall station (RF) Ldg. Dominion (RF 3018107) as station 2. The missing rainfall data of station 2 is estimated using the normal ratio method from the observations of rainfall at some of the other stations, as close to and as evenly spaced around the station with the missing record as possible [39].

2.6.3. Distribution of Rainfall and Water Level

The mean and median values were estimated for 30 years of raw data, from October 1986 to September 2016, and are presented in Figure 4. The most likely time for drought to happen is when the rainfall is low. It can be seen that, for the distribution of the rainfall data for station 2, the highest mean and median were in November, at 369.4 mm and 317.0 mm, respectively. The lowest rainfall was in January, with a mean of 138.4 mm and median of 126.3 mm, followed by June, July, and February. There are basically three different seasons in the Langat River Basin of Malaysia. The wet period of the year is from October through to the beginning of January, and the dry months are generally observed

from January to March, and June to September. October and November are the wettest months, with an average rainfall of 321.5 mm and 369.4 mm, respectively.

Figure 5 presents the water level data of station 1, and it can be seen that the water level steadily decreased for the second half of the duration of this study.

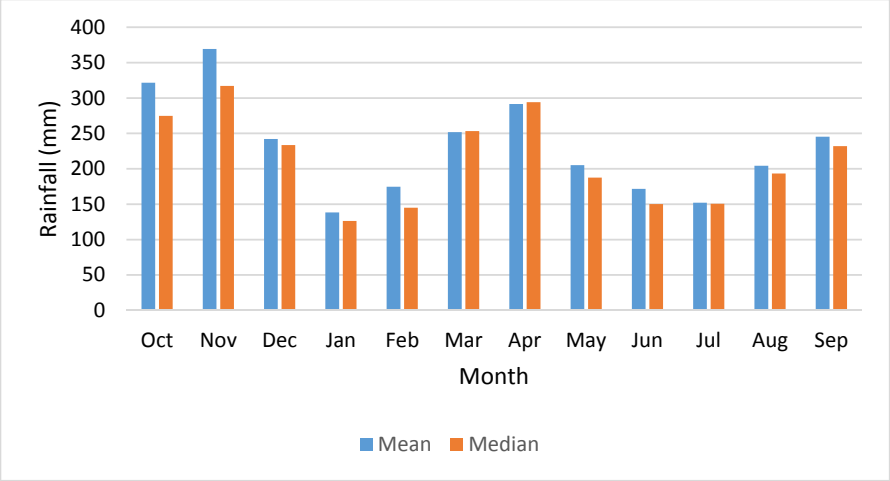

Figure 4. Monthly rainfall distribution at station 2, estimated using data from 1986 to 2016.

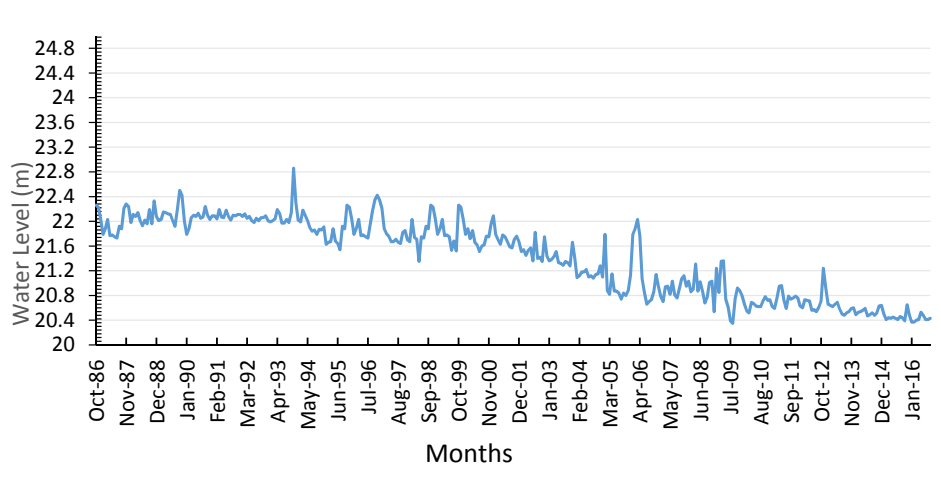

Figure 5. Water level data for 30 years at station 1 (1986–2016).

3. Results and Discussion

3.1. Assessment Using Standard Index of Annual Precipitation (SIAP)

As illustrated in Figure 6, the highest SIAP value was 4.921 (October 1994) and the lowest value was −1.591 (August 1990). In 1988, the drought period was 11 months; followed by 1990, with a drought period of 10 months; and then 2015, with a nine month dry period. Figure 6 also shows that in 1988, there was a 10 month dry period from March to December.

Figure 7 shows a categorization of the results for the five different classes of drought. It shows that 17% of the months were extremely wet, 7% were wet, 39% were normal, 17% had drought, and 20% had very severe drought. Overall, drought happened during 37% of the total months, and wet periods occurred during 24% of the total months. Table 4 shows a summary of the drought classifications.

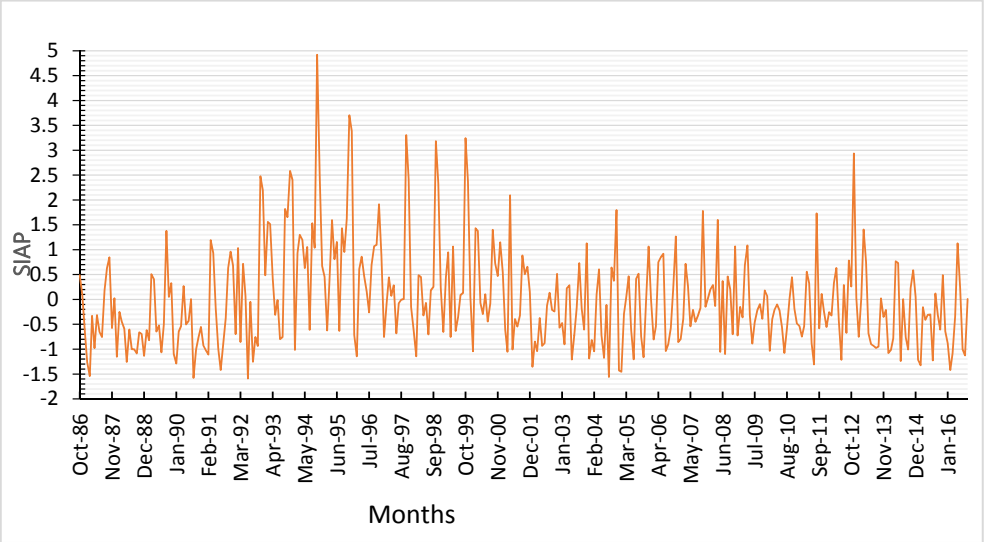

Figure 6. Standard Index of Annual Precipitation (SIAP) values for 30 years at station 2.

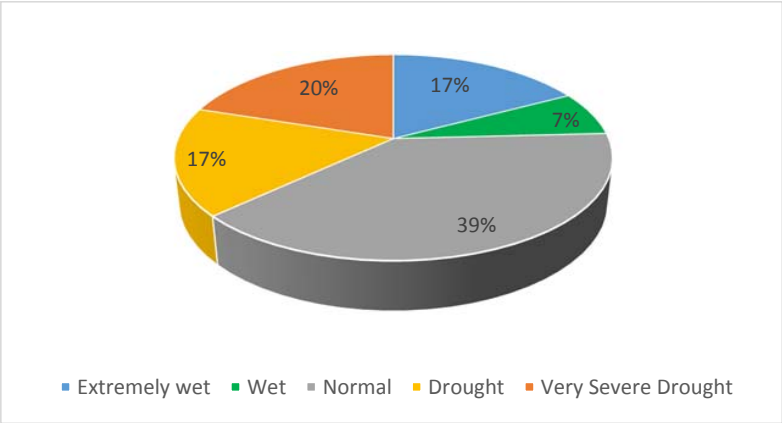

Figure 7. Distribution of SIAP values into classes (station 2).

Table 4. Summary of drought classifications for station 2.

Category	Number of Months	Percentage (%)
Extremely wet	62	17
Wet	25	7
Normal	140	39
Drought	61	17
Very severe drought	72	20
Total	360	100

Artificial Neural Network (ANN) Model

The ANN architecture does not have a systematic way to establish suitable architecture. Networks that are too small and simple can lead to underfitting, while networks that are too complex tend to overfit the training pattern [40]. Usually, nonlinear sigmoidal activation functions are used, as reported in the literature, which were also adopted in this study. The inputs to the ANN model were normalized and kept within the range of 0.1 to 0.9. Normalization or scaling is not really a functional requirement for the NNs to learn, but it significantly helps as it transposes the input variables into the data range that the sigmoid activation functions lie in (i.e., 0.1). The learning rate and momentum coefficient

are influential parameters that control the convergence rate, but optimize them for the best output. Here, the two parameters were kept constant at 0.4 and 0.6, respectively, throughout the network structure for various numbers of hidden neurons. The network input models that were tested for the forecasting were based on the SIAP at station 2, shown by Equations (11) and (12). The input combinations consisted of lagged data of the rainfall and drought index, and the output was kept as a single drought index variable.

$$\text{SIAP (t)} = \text{f } (R_{t-1}, R_{t-2}, R_{t-3}) \quad \text{Input model number 1} \tag{11}$$

$$\text{SIAP (t)} = \text{f } (SI_{t-1}, SI_{t-2}, SI_{t-3}) \quad \text{Input model number 2} \tag{12}$$

where SIAP or SI is the drought index; R is the precipitation; *n* is the time lag, which is effectively the lead time of the forecast; and t is time in months. The input models based on the main parameter, rainfall, in calculating the index or a drought index itself as input, performed better in the forecasting using ANN [41]. The same study also illustrated a lack of impact of the secondary parameters on the performance of the networks. In the ANN model stated above, there are three classifications of samples, training, which was kept at 70% (252 samples); validation, 15% (54 samples); and testing, 15% (54 samples). In the majority of the cases, data division is carried out on an arbitrary basis. However, the way the data divided can have a significant effect on the model performance. Shahin et al. [42] investigated the issue of data division and its impact on the ANN model performance for a case study of predicting the settlement of shallow foundations on granular soils. The results indicated that the statistical properties of the data in the training, testing, and validation sets need to be taken into account in order to ensure that the optimal model performance is achieved [42]. During training, it adjusts the network according to its final measured error. The validation process was used at the end of training as an extra check on the performance of the model. If the performance of the network was found to be consistently good on both the test and the validation samples, then it was reasonable to assume that the network would generalize well on unseen data. For testing, this does not affect the training part, but it provides an independent measure of the network performance during and after training. Each MLP was trained with 5 to 15 hidden neurons in a single hidden layer, as shown in Table 5, to select the most effective model by analyzing the performance. The three best-performing combinations are shown for each input model.

Table 5. Correlation coefficient (R) of artificial neural network (ANN) network structure (SIAP).

Input Model Number	Number of Neurons	R			
		Training	Validation	Testing	Overall
1	10	0.907	0.865	0.908	0.899
1	15	0.803	0.845	0.758	0.800
1	12	0.796	0.765	0.801	0.783
2	8	0.712	0.813	0.705	0.741
2	9	0.737	0.799	0.782	0.770
2	10	0.882	0.875	0.851	0.868

For the comparison between the output and target, it was found that for input model number 1, for training, validation, testing, and overall, the R values were 0.907, 0.865, 0.909, and 0.899, respectively. An R value of 1 means a close relationship, 0 means no relationship. So, this means that the relationship between the two (output and target) are close and related, which is shown in Figure 8. The errors in the training, validation, and testing stages are illustrated in Figure 9.

Figure 10 displays a section of time series from January 1987 to December 1989 of the SIAP observed values against the forecasted ones, by using input model number 1. The results effectively exemplify the high accuracy of the short-range forecasts of the droughts at station 2. Such studies may be a way to identify the operational accuracy of forecasts, and have been used by others for similar purposes [43].

The forecasted and actual index values were similar, so the model can be said to be reliable. Therefore, this ANN model can be used to predict short- to medium-term drought occurrences in Malaysia. In addition, SIAP is an effective index for the assessment of drought monitoring and the characteristics of drought conditions in the Langat River Basin. Authorities can render early warnings for the timely implementation of preparedness based on predictions.

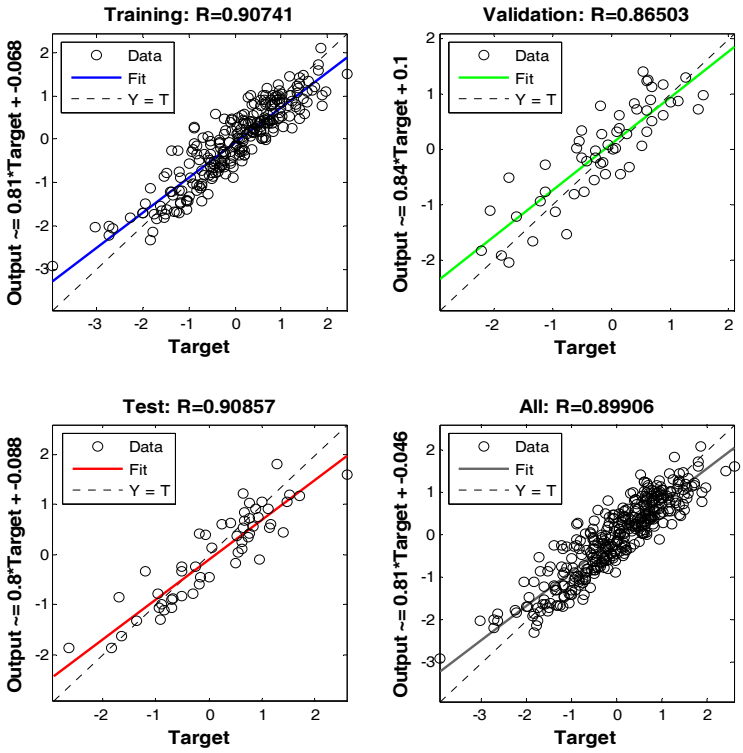

Figure 8. Neural network training regression for input model 1.

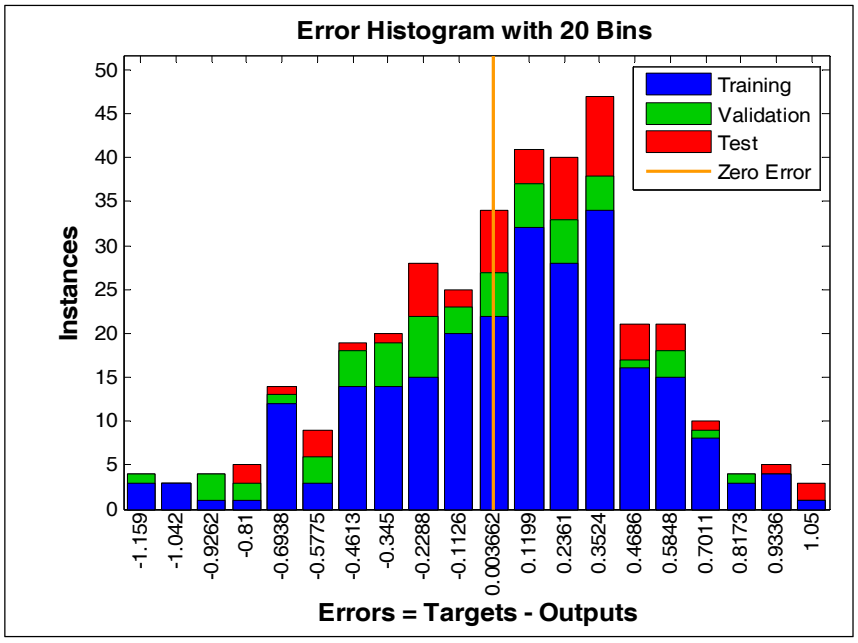

Figure 9. Error histogram of input model number 1.

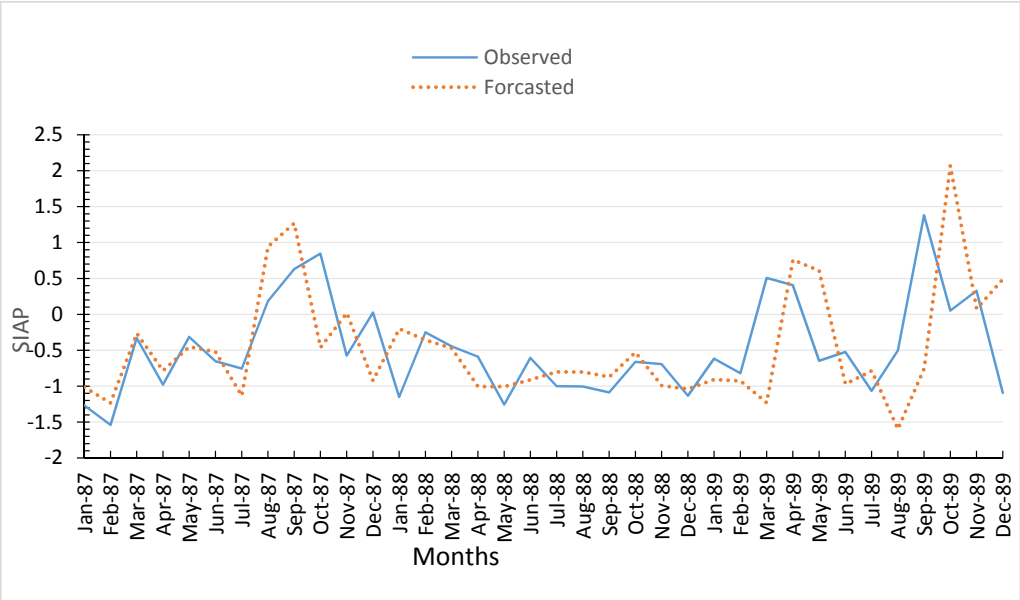

Figure 10. Comparison of observed and forecasted SIAP at station 2 of input model number 1.

3.2. Assessment Using SWSI for Hydrological Drought

Figure 11 shows the time series created using SWSI for the 30 years of data at station 1. The data used for the analysis was the water level of the river. Initially, the values are seen to be classified as very wet or above, then, they slowly change to near normal. The trend of SWSI in Figure 11 is similar to the raw input water level data, seen in Figure 5, which shows that almost the first half of the whole period was very wet or above normal, and the second half was below normal or had droughts. Climate change, rapid urbanization, environmental degradation, and industrial development may have resulted in water and related resources within the basin becoming increasingly stressed. A study conducted in Malaysia highlighted that extreme dry conditions are becoming more frequent than extreme wet conditions [5]. With reference to Figure 5, the time series starts with one month of moderately wet conditions, which follows 12 months of near-normal conditions. From November 1987 to May 1994 (months 14 to 92), the conditions are classified as very wet, extremely wet, or moderately wet. After this wet period, the values are observed to decrease gradually, from very wet conditions to near normal conditions. From June 1994 to November 2008 (months 93 to 266), the conditions were near normal. However, there were few months that were moderately wet, very wet, or extremely wet. The first drought occurred in December 2008 (month 267), with an index value of −1.39. Drought started to occur more frequently from this point onward. Near-normal conditions are observed from January 2009 (month 268) to February 2013 (month 317). However, within this period, the months with drought increased. From March 2013 (month 318) to September 2016 (month 360), all of the months experienced drought. The most frequent type of drought was moderate drought, followed by extreme drought. The number of occurrences of severe drought is less than that of moderate and extreme drought.

Table 6 shows the number of months that each drought occurred, with percentages varying from 2.50% to 66.67%. The most observed condition within the period of study was near normal. Near normal conditions occurred for 240 months, about 66.67%. Except for the near normal, all of the other conditions were below 11%. Moderate drought occurred for 37 months (10.28%). Moderately wet conditions occurred for a similar number of months (35 months; 9.72%). Very wet conditions were observed in 16 months (4.44%), followed by extremely wet conditions in 12 months (3.33%). Extreme drought occurred in 11 months (3.06%). The least frequent condition was severe drought, which occurred in 9 months (2.5%).

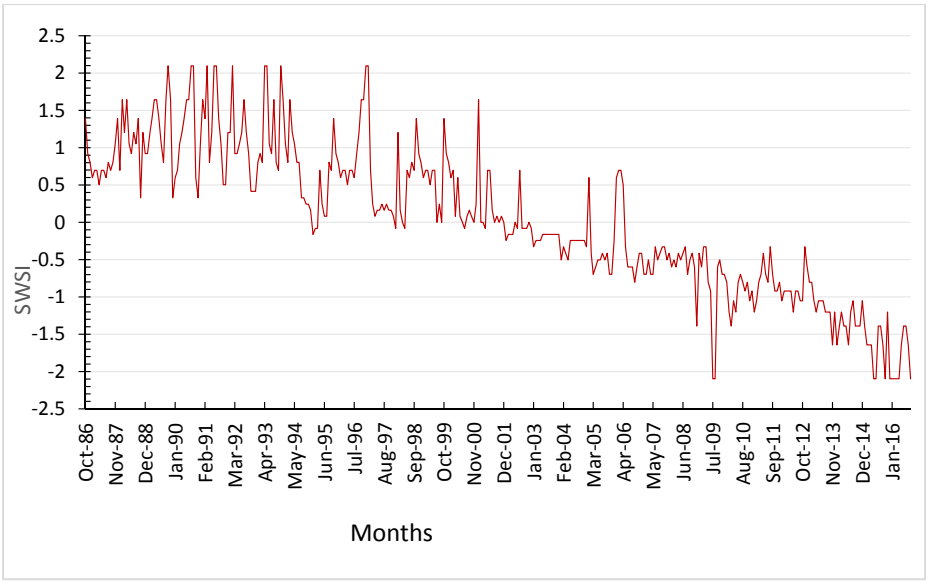

Figure 11. Standardized Water Storage Index (SWSI) values for station 1 for 30 years (360 months).

Table 6. SWSI drought percentage from station 1.

Drought Classification	Condition	Number of Months	Percentage (%)
Extremely wet	>2	12	3.33
Very wet	1.5 to −2	16	4.44
Moderately wet	1.0 to 1.5	35	9.72
Near normal	−1.0 to 1.0	240	66.67
Moderate drought	−1.5 to −1.0	37	10.28
Severe drought	−2.0 to −1.5	9	2.50
Extreme drought	<−2	11	3.06

Artificial Neural Network Model for Hydrological Drought

The network input models that were tested are based on SWSI at station 1, shown by Equations (13) and (14), as follows:

$$\text{SWSI}(t) = f(W_{t-1}, W_{t-2}, W_{t-3}) \quad \text{Input model number 3} \tag{13}$$

$$\text{SWSI}(t) = f(SW_{t-1}, SW_{t-2}, SW_{t-3}) \quad \text{Input model number 4} \tag{14}$$

where SWSI or SW is the drought index, W is the water level, and n is the time lag, which is effectively the lead time of the forecasted SWSI model developed for station 1. Similar to the SIAP ANN model, in this case as well, each MLP was trained with 5 to 15 hidden neurons in a single hidden layer, as shown in Table 7, in order to select the most effective model by analyzing performance. The three best-performing combinations are shown for each input model.

Table 7. Correlation coefficient (R) of ANN network structure (SWSI).

Input Model Number	Number of Neurons	R			
		Training	Validation	Testing	Overall
3	10	0.968	0.967	0.969	0.968
3	11	0.898	0.908	0.951	0.918
3	7	0.767	0.801	0.822	0.796
4	15	0.901	0.855	0.835	0.865
4	10	0.911	0.899	0.853	0.888
4	6	0.751	0.772	0.811	0.779

The output, which is the forecasted results, is plotted together with the observed results in Figure 12, using the SWSI input model (number 3). The dotted line shows the forecasted values and the solid line shows the observed results, which were calculated by SWSI. In general, the two plots are not very different. The forecasted values have only minor differences.

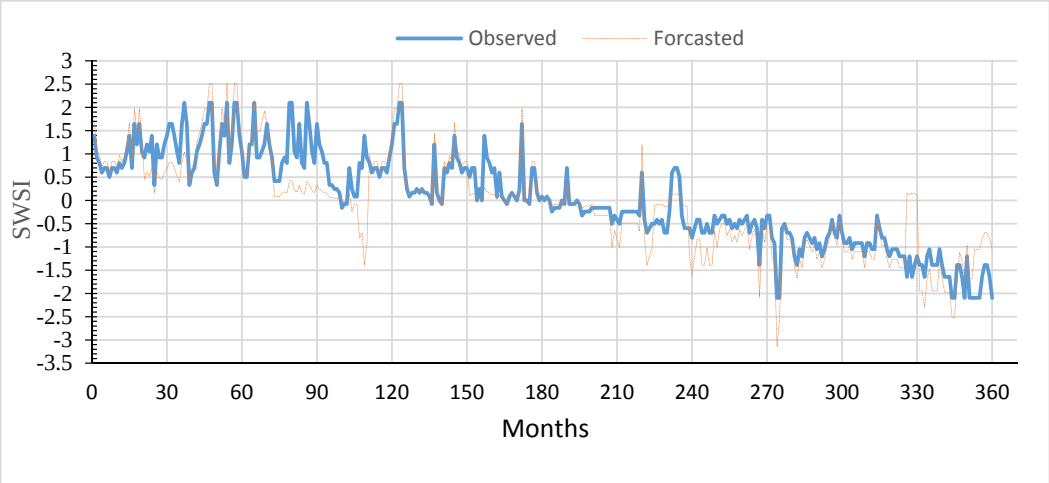

Figure 12. SWSI observed and forecasted values (360 months) of station 1 for input model number 3.

An error histogram for input model number 3 of SWSI was also plotted, and is shown in Figure 13. The error histogram assists in authenticating the performance of the network. The blue part represents the training data and the green part represents the validation data. The biggest portion of data is surrounding the zero line. The zero line offers a way to confirm the outliers to determine if the data contains errors. It can also confirm that those data features are not like the leftovers of the dataset [44].

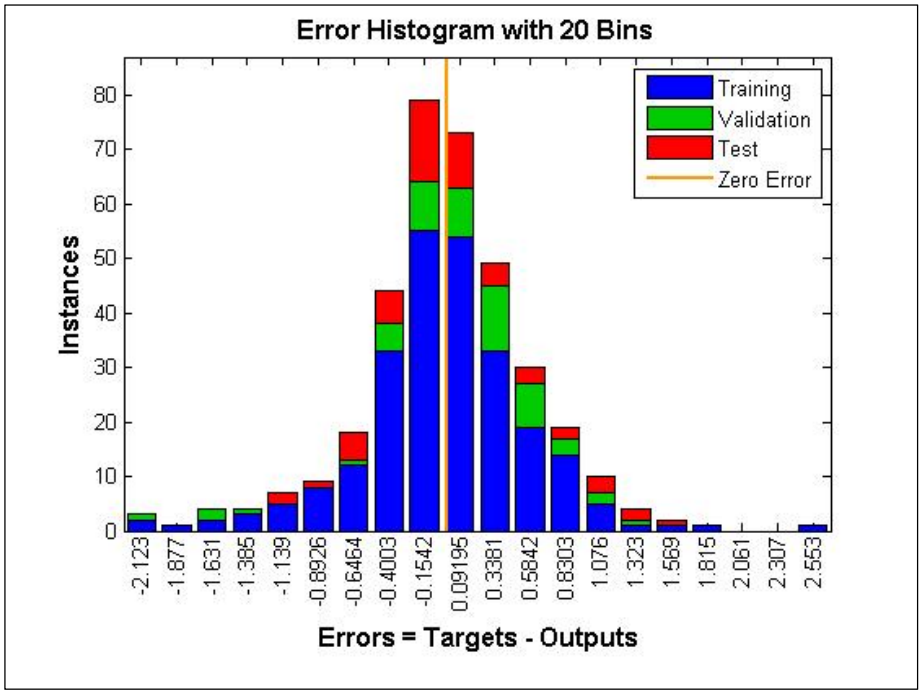

Figure 13. Error histogram for SWSI input model number 3.

The R value shown in Figure 14 concludes the connection between the output or target values of the artificial neural network models. The R value is also known as the correlation coefficient. Strong and random connections were identified when the R value was 1 and 0, respectively [45]. The line must be at a 45° angle toward 1 to be a perfect fit. The 45° line means that the output value is equal to the input target values. For SWSI, the R values for training, validation, testing, and overall, are the same at 0.96. This indicates a strong correlation in the prediction of drought, based on the observed values and developed model [44].

A time series of the calculated indices plotted shows that drought is not increasing gradually, but occurs irregularly. The water level decreased and drought increased gradually every year. SWSI considers values between +1 and −1 as near normal, whereas other hydrological drought indices (e.g., SDI) consider all of the values below 0 as drought.

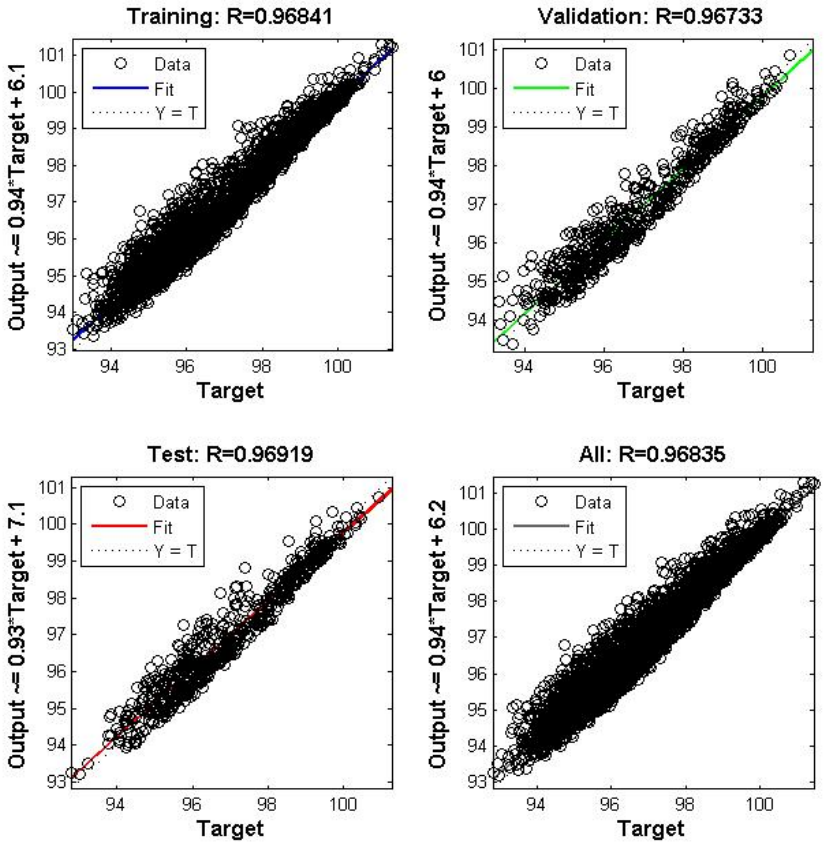

Figure 14. Correlation coefficient for SWSI at station 1 for input model number 3.

3.3. W-ANN Model

As seen in Table 8, there is a correlation between the DWT wavelet components D1, D2, D3, D4, D5, D6, D7, and D8 of the SIAP, SWSI, rainfall, and water level series, with the original series. It can be observed, in the case of SIAP, SWSI, and rainfall, that D1, D2, D3, and D8 show significantly higher correlations than the average of correlations among them compared to the D4, D5, and D6 components. However, for the water level, only D7 and D8 subseries show higher than average correlations. According to the correlation analysis, the effective components were selected as the dominant wavelet components, as stated above. Afterwards, the significant wavelet components and the approximation (A8) component were added to constitute the new series.

Table 8. The correlation coefficient between each sub-time series and original drought indices/raw input series.

Discrete Wavelet Components (db3)	Correlation between Detailed Sub-Time Series and Observed Drought Index/Rainfall/Water Level Data				
	SIAP	**SWSI**	**Rainfall**	**Water Level ***	**Dominant**
D1	0.5291	0.1996	0.5291	0.1335	√
D2	0.5732	0.2221	0.5732	0.1522	√
D3	0.3645	0.1900	0.3645	0.1409	√
D4	0.2130	0.1322	0.2130	0.1120	x
D5	0.1616	0.1519	0.1616	0.1333	x
D6	0.2576	0.1885	0.2576	0.0694	x
D7	0.2015	0.0820	0.2015	0.3151 *	
D8	0.3201	0.3923	0.3201	0.4303 *	√
Average	0.3274	0.1948	0.3274	0.1858	

* Only D7 and D8 subseries show higher than average correlations. √ indicates that the subseries is dominant; x indicates that the subseries is not dominant.

Secondly, the W-ANN models were developed for monthly drought prediction, using wavelet subseries. The most important part of this wavelet-based model is the selection of inputs for its formation. The summed wavelet components (the new series) instead of the original data were employed as inputs of the W-ANN model for drought prediction. Four different models based on combinations of different input data (SIAP, SWSI, rainfall, and water level) were evaluated. The forecasting performance of the wavelet–neural network models are presented in Table 9, in terms of RMSE and R. The table shows that the W-ANN model has a significant positive effect on the monthly drought forecast. As seen from the table, model number 4, with three months of previous SWSI data, has the lowest RMSE and the highest correlation coefficients among all of the wavelet–neural network models. For meteorological drought prediction, while the highest correlation coefficient (R) obtained by the ANN model is 0.899, with the wavelet-ANN model, this value increased to 0.940. Similarly, for the case of hydrological drought, while the R obtained by the ANN model is 0.968, with the wavelet-ANN model, this value increased to 0.973. The application of wavelet in the ANN model achieved higher correlation coefficients for all of the models, except for input model number 3. In both types of drought forecasting, it was found that the models based on preceding drought index values as inputs performed better than the models developed with raw data, such as rainfall or water level as inputs. This proves that the created models can improve hydrologic and meteorological drought prediction close to the observed values.

Table 9. Root mean-square error (RMSE) and R statistics of different W-ANN models.

Input Model (After Wavelet Decomposition)	RMSE (Validation)	R (Overall)	Hidden Neurons
1 (R_{t-1}, R_{t-2}, R_{t-3})	0.38	0.932	8
1 (R_{t-1}, R_{t-2}, R_{t-3})	0.41	0.931	10
1 (R_{t-1}, R_{t-2}, R_{t-3})	0.38	0.901	15
2 (SI_{t-1}, SI_{t-2}, SI_{t-3})	0.40	0.922	8
2 (SI_{t-1}, SI_{t-2}, SI_{t-3})	0.42	0.931	10
2 (SI_{t-1}, SI_{t-2}, SI_{t-3})	0.39	0.940	15
3 (W_{t-1}, W_{t-2}, W_{t-3})	0.40	0.902	8
3 (W_{t-1}, W_{t-2}, W_{t-3})	0.43	0.901	10
3 (W_{t-1}, W_{t-2}, W_{t-3})	0.38	0.910	15
4 (SW_{t-1}, SW_{t-2}, SW_{t-3})	0.19	0.971	10
4 (SW_{t-1}, SW_{t-2}, SW_{t-3})	0.17	0.972	13
4 (SW_{t-1}, SW_{t-2}, SW_{t-3})	0.21	0.973	15

Table 10 shows the performance improvement of the W-ANN models, and it can be seen that the models for meteorological drought forecasting improved by 3.67% and 8.29%; however, for the hydrological drought forecasting models, there was a decrease of R value by 5.99% for input model number 3. Input model number 4 performed better than the other models that were considered in this study, with a performance improvement of 9.57%.

Table 10. Performance improvement of R statistics of different W-ANN models.

Input Model	R (With Wavelet Decomposition)	R (Without Wavelet Decomposition)	Performance Improvement (%)
1 (R_{t-1}, R_{t-2}, R_{t-3})	0.932	0.899	+3.67
2 (SI_{t-1}, SI_{t-2}, SI_{t-3})	0.940	0.868	+8.29
3 (W_{t-1}, W_{t-2}, W_{t-3})	0.910	0.968	−5.99
4 (SW_{t-1}, SW_{t-2}, SW_{t-3})	0.973	0.888	+9.57

Figure 15 shows a scatter plot using model number 4 (SWSI), and it shows that the W-ANN forecasts approximate the general behavior of the observed data more satisfactorily for the drought months.

Figure 16 shows a scatter plot using model number 3 (SIAP), and it shows that the W-ANN forecasts do not linearly approximate the general behavior of the observed data, but the correlation coefficient is 0.940.

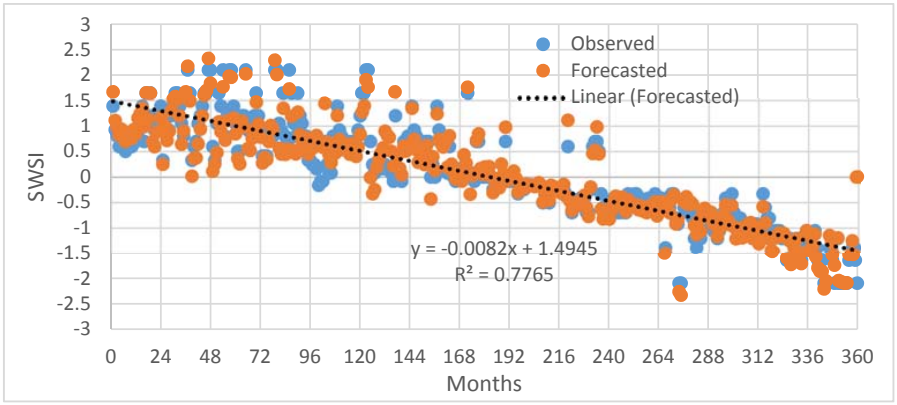

Figure 15. Scatter plot comparing observed and forecasted hydrological drought using W-ANN models.

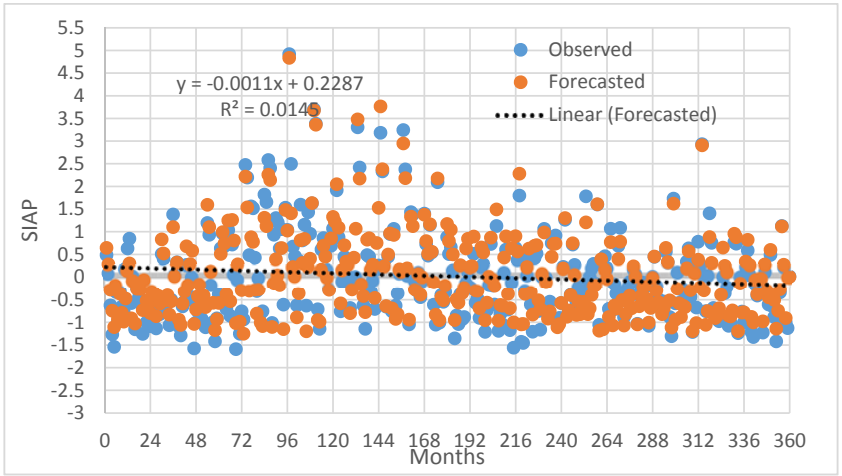

Figure 16. Scatter plot comparing observed and forecasted meteorological drought using W-ANN models.

4. Conclusions

Drought occurrences in the Langat River catchment of peninsular Malaysia were characterized using meteorological and hydrological drought indices, SIAP and SWSI, respectively. Overall, SWSI and SIAP were found to be effective indices for the assessment of drought. The occurrence of hydrological and meteorological droughts was found to be around 16% and 37% by SWSI and SIAP, respectively. Two neural network-based models and two wavelet-based ANN models were developed using the values of SIAP and SWSI. For SWSI and SIAP, correlation coefficients of 0.96 and 0.90, respectively, were calculated. Therefore, it is concluded that both of the models are found to be reliable. However, with the W-ANN model, these values increased to 0.940 and 0.973 for meteorological and hydrological drought forecasting, respectively. This proves that the proposed models are able to predict hydrologic and meteorological drought very close to the observed values. This study can help in the drought assessment and the prediction of drought occurrence in the study area. Authorities can issue an early warning for the timely implementation of preparedness, based on predictions.

Author Contributions: M.M.H.K. designed the research, carried out the analysis, and wrote the article. N.S.M. and A.E.-S. helped to conceive the research, review the overall results, and initiate the article. All of the authors contributed substantially to the work reported.

Funding: Fundamental Research Grant Scheme (Grant No. FRGS/2/2014/TK02/UKM/03/2), provided by the Ministry of Education Malaysia

Acknowledgments: The authors would like to acknowledge support from the Ministry of Education (MOE) and the Universiti Kebangsaan Malaysia (UKM) for research grant FRGS/2/2014/TK02/UKM/03/2. They also acknowledge contributions from Adil Rassam Timimi and Ahmed Ali Jabir at the University of Nottingham, Malaysia, for help with the analysis. Appreciation is due to the Department of Irrigation and Drainage (DID) for the data supplied to conduct this research study.

Conflicts of Interest: The authors declare no conflict of interest.

References

1. Basics, D.; Drought, T. Types of Drought. Available online: http://drought.unl.edu/DroughtBasics/TypesofDrought.aspx (accessed on 14 October 2017).
2. Deni, S.; Jemain, A.; Ibrahim, K. The spatial distribution of wet and dry spells over Peninsular Malaysia. *Theor. Appl. Climatol.* **2008**, *94*, 163–173. [CrossRef]
3. Jamalluddin, S.A.; Low, K.S. Droughts in Malaysia: A Look at Its Characteristics, Impacts, Related Policies and Management Strategies. In Proceedings of the Water and Drainage 2003 Conference, Kuala Lumpur, Malaysia, 28–29 April 2003.
4. Staff, S.; Staff, S. Drought beyond India: Malaysia Faces a Massive Water Crisis as South East Asia Swelters. Available online: http://scroll.in/article/806812/drought-beyond-india-malaysia-faces-a-massive-water-crisis-as-south-east-asia-swelters (accessed on 25 November 2017).
5. Wan, W.Z.; Ibrahim, K.; Jemain, A.A. Evaluating dry conditions in Peninsular Malaysia using bivariate copula. *Anziam J.* **2010**, *51*, 555–569.
6. Morid, S.; Smakhtin, V.; Moghaddasi, M. Comparison of seven meteorological indices for drought monitoring in Iran. *Int. J. Climatol.* **2006**, *26*, 971–985. [CrossRef]
7. Karavitis, C.A.; Alexandris, S.; Tsesmelis, D.E.; Athanasopoulos, G. Application of the Standardized Precipitation Index (SPI) in Greece. *Water* **2011**, *3*, 787–805. [CrossRef]
8. Gourabi, B.R. The Recognition of Drought with Dri and Siap Method and its Effects on Rice Yield and Water Surface in Shaft, Gilan, south Western of Caspian Sea. *Aust. J. Basic Appl. Sci.* **2010**, *4*, 4374–4378.
9. Arvind Singh, T.; Bhawana, N.; Lokendra, S. Drought spells identification with indices for Almora district of Uttarakhand, India. *Am. Int. J. Res. Sci. Technol. Eng. Math.* **2015**, *12*, 1–5.
10. Farahmand, A.; AghaKouchak, A. A generalized framework for deriving nonparametric standardized drought indicators. *Adv. Water Resour.* **2015**, *76*, 140–145. [CrossRef]
11. Wang, W.; Wang, P.; Cui, W. A comparison of terrestrial water storage data and multiple hydrological data in the Yangtze River basin. *Adv. Water Sci.* **2015**, *26*, 759–768.

12. Nourani, V.; Komasi, M.; Mano, A. A Multivariate ANN-Wavelet Approach for Rainfall–Runoff Modeling. *Water Resour. Manag.* **2009**, *23*, 2877. [CrossRef]
13. Panagoulia, D. Hydrological modeling of a medium-sized mountainous catchment from incomplete meteoro-logical data. *J. Hydrol.* **1992**, *137*, 279–310. [CrossRef]
14. Panagoulia, D. Artificial neural networks and high and low flows in various climate regimes. *Hydrol. Sci. J.* **2006**, *51*, 563–587. [CrossRef]
15. Govindaraju, R. Artificial neural networks in hydrology. II: hydrologic applications. *J. Hydrol. Eng.* **2000**, *5*, 124–137.
16. Peng, T.; Zhou, J.; Zhang, C.; Fu, W. Streamflow Forecasting Using Empirical Wavelet Transform and Artificial Neural Networks. *Water* **2017**, *9*, 406. [CrossRef]
17. Zhou, J.; Peng, T.; Zhang, C.; Sun, N. Data Pre-Analysis and Ensemble of Various Artificial Neural Networks for Monthly Streamflow Forecasting. *Water* **2018**, *10*, 628. [CrossRef]
18. Remesan, R.; Shamim, M.A.; Han, D.; Mathew, J. Runoff prediction using an integrated hybrid modelling scheme. *J. Hydrol.* **2009**, *372*, 48–60. [CrossRef]
19. Tayyab, M.; Zhoua, J.; Adnana, R.; Zenga, X.; Zenga, X. Application of Artificial Intelligence Method Coupled with Discrete Wavelet Transform Method. *Procedia. Comput. Sci.* **2017**, *107*, 212–217. [CrossRef]
20. Zhou, T.; Wang, F.; Yang, Z. Comparative Analysis of ANN and SVM Models Combined with Wavelet Preprocess for Groundwater Depth Prediction. *Water* **2017**, *9*, 781. [CrossRef]
21. Seo, Y.; Choi, Y.; Choi, J. River Stage Modeling by Combining Maximal Overlap Discrete Wavelet Transform, Support Vector Machines and Genetic Algorithm. *Water* **2017**, *9*, 525.
22. Wang, D.; Ding, J. Wavelet network model and its application to the prediction of hydrology. *Nat. Sci.* **2003**, *1*, 67–71.
23. Kim, T.W.; Valdes, J.B. Nonlinear model for drought forecasting based on a conjunction of wavelet transforms and neural networks. *J. Hydrol. Eng.* **2003**, *6*, 319–328. [CrossRef]
24. Shabri, A. A hybrid model for stream flow forecasting using wavelet and least Squares support vector machines. *Jurnal Teknologi* **2015**, *73*, 89–96. [CrossRef]
25. Belayneh, A.; Adamowski, J. Drought forecasting using new machine learning methods. *J. Water Land Dev.* **2013**, *18*, 3–12. [CrossRef]
26. Khalili, A.; Bazrafshan, J. Assessing the efficiency of several drought indices in different climatic regions of Iran. *Nivar J.* **2003**, *48*, 79–93.
27. Najjar, S.; Rouhollah, R.Y. Studying & Comparing the Efficiency of 7 Meteorological Drought Indices in Droughts Risk Management (Case Study: North West Regions). *Appl. Math. Eng. Manag. Technol.* **2015**, *3*, 131–142.
28. Haykin, S. *Neural Networks: A Comprehensive Foundation*, 2nd ed.; Prentice Hall: Upper Saddle River, NJ, USA, 1999.
29. Demuth, H.; Beale, M. *Neural Network Toolbox: For Use with Matlab*; The MathWorks, Inc.: Natick, MA, USA, 2005.
30. Bishop, C.M. *Neural Networks for Pattern Recognition*; Oxford University Press: Oxford, UK, 1995; p. 482.
31. El-Shafie, A.; Noureldin, A.; Taha, M.; Hussain, A. Dynamic versus static neural network model for rainfall forecasting at Klang River Basin, Malaysia. *Hydrol. Earth Syst. Sci. Discuss.* **2011**, *8*, 6489–6532. [CrossRef]
32. Dawson, C.W.; Abrahart, R.J.; See, L.M. HydroTest: A web-based toolbox of statistical measures for the standardised assessment of hydrological forecasts. *Environ. Modell. Softw.* **2007**, *27*, 1034–1052. [CrossRef]
33. Napolitano, G.; Serinaldi, F.; See, L. Impact of EMD decomposition and random initialisation of weights in ANN hindcasting of daily stream flow series: An empirical examination. *J. Hydrol.* **2011**, *406*, 199–214. [CrossRef]
34. Barua, S.; Ng, A.; Perera, B. Artificial Neural Network—Based Drought Forecasting Using a Nonlinear Aggregated Drought Index. *J. Hydrol. Eng.* **2012**, *17*, 1408–1413. [CrossRef]
35. Kisi, O. Wavelet regression model as an altrnative to neural networks for river stage forecasting. *Water Resour. Manag.* **2011**, *25*, 579–600. [CrossRef]
36. Nourani, V.; Baghanam, A.H.; Adamowski, J.; Kisi, O. Applications of hybrid wavelet-Artificial Intelligence models in hydrology: A review. *J. Hydrol.* **2014**, *514*, 358–377. [CrossRef]
37. Mallat, S.G. A theory for multi decomposition signal decomposition: The wavelet representation. *IEEE Trans. Pattern Anal. Mach. Intell.* **1989**, *11*, 674–693. [CrossRef]

38. Hasan, M.; Begum, M.; Al Mamun, A.; Haque Khan, Z. Selection of extreme drought event for Langat Basin and its consequence on salinity intrusion through Langat River System. *IOSR J. Mech. Civ. Eng.* **2014**, *11*, 62–69. [CrossRef]
39. Singh, V.P. *Elementary Hydrology*; Prentice Hall of India: New Delhi, India, 1994.
40. Dawson, C.W.; Abrahart, R.J.; Shamseldin, A.Y.; Wilby, R.C. Flood estimation at ungauged sites using artificial neural networks. *J. Hydrol.* **2006**, *319*, 391–409. [CrossRef]
41. Morid, S.; Smakhtin, V.; Bagherzadeh, K. Drought forecasting using artificial neural networks and time series of drought indices. *Int. J. Climatol.* **2007**, *27*, 2103–2111. [CrossRef]
42. Shahin, M.A.; Maier, H.R.; Jaksa, M.B. Data Division for Developing Neural Networks Applied to Geotechnical Engineering. *J. Comput. Civ. Eng.* **2004**, *18*, 105–114. [CrossRef]
43. Khadr, M. Forecasting of meteorological drought using Hidden Markov Model (case study: The upper Blue Nile river basin, Ethiopia). *Ain Shams Eng. J.* **2016**, *7*, 47–56. [CrossRef]
44. Claudio, G.; Joseph, Q.; Carmine, T.; Svetoslav, I.; Silviya, P. Public Transportation Energy Consumption Prediction by means of Neural Network and Time Series Analysis Approaches. In Proceedings of the 6th International Conference on Automotive and Transportation Systems, Slerno, Italy, 27–29 June 2015; pp. 64–70.
45. Amit, K.Y.; Hasmat, M.; Chandel, S.S. Selection of most relevant input parameters using WEKA for artificial Neural network based solar radiation prediction models. *Renew. Sustain. Energy Rev.* **2014**, *31*, 509–519.